Enzyme Catalysis and Regulation:

Rapid Kinetics of Na^+ Binding to Thrombin

Alaji Bah, Laura C. Garvey, Jingping Ge and Enrico Di Cera

J. Biol. Chem. 2006, 281:40049-40056.
doi: 10.1074/jbc.M608600200 originally published online October 30, 2006

THE JOURNAL OF BIOLOGICAL CHEMISTRY VOL. 281, NO. 52, pp. 40049–40056, December 29, 2006

Rapid Kinetics of Na^+ Binding to Thrombin*[S]

Received for publication, September 6, 2006, and in revised form, October 30, 2006 Published, JBC Papers in Press, October 30, 2006, DOI 10.1074/jbc.M608600200

Alaji Bah, Laura C. Garvey, Jingping Ge, and Enrico Di Cera[1]

From the Department of Biochemistry and Molecular Biophysics, Washington University School of Medicine, St. Louis, Missouri 63110

The kinetic mechanism of Na^+ binding to thrombin was resolved by stopped-flow measurements of intrinsic fluorescence. Na^+ binds to thrombin in a two-step mechanism with a rapid phase occurring within the dead time of the spectrometer (<0.5 ms) followed by a single-exponential slow phase whose k_{obs} decreases hyperbolically with increasing [Na^+]. The rapid phase is due to Na^+ binding to the enzyme *E* to generate the *E*:Na^+ form. The slow phase is due to the interconversion between *E and *E*, where *E** is a form that cannot bind Na^+. Temperature studies in the range from 5 to 35 °C show significant enthalpy, entropy, and heat capacity changes associated with both Na^+ binding and the *E* to *E** transition. As a result, under conditions of physiologic temperature and salt concentrations, the *E** form is negligibly populated (<1%) and thrombin is almost equally partitioned between the *E* (40%) and *E*:Na^+ (60%) forms. Single-site Phe mutations of all nine Trp residues of thrombin enabled assignment of the fluorescence changes induced by Na^+ binding mainly to Trp-141 and Trp-215, and to a lesser extent to Trp-148, Trp-207, and Trp-237. However, the fast phase of fluorescence increase is influenced to different extents by all Trp residues. The distribution of these residues over the entire thrombin surface demonstrates that Na^+ binding induces long-range effects on the structure of the enzyme as a whole, contrary to the conclusions drawn from recent structural studies. These findings elucidate the mechanism of Na^+ binding to thrombin and are relevant to other clotting factors and enzymes allosterically activated by monovalent cations.**

Numerous enzymes with widely different functions, structures, and mechanisms require a monovalent cation (M^+) for optimal catalytic activity (1–3). In practically all cases reported to date, M^+ activation is mediated by Na^+ or K^+ with high selectivity (3, 4). Remarkable progress has been made during the past decade in the structural characterization of such enzymes. Structural studies have uncovered two basic mechanisms of activation, one in which M^+ functions as a cofactor by bridging atoms of the protein and substrate in the active site and another in which M^+ binds away from substrate and influences recognition and catalysis through an allosteric mechanism. A simple classification of M^+-activated enzymes has been proposed recently by merging information from kinetic and structural studies (3). The classification groups enzymes based on their M^+ specificity (Na^+ or K^+) and the mechanism of activation, cofactor-like (Type I) or allosteric (Type II).

Among Na^+-activated Type II enzymes, thrombin has been studied in considerable detail both functionally and structurally (5–7). Na^+ binds near the primary specificity pocket, nestled between the 186 and 220 loops (8, 9), and is required for efficient cleavage of the procoagulant factors fibrinogen (10), factors V (11), VIII (12), XI (13), and the prothrombotic factor PAR1 (14), but not for activation of the anticoagulant protein C (10, 15). Hence, Na^+ binding to thrombin controls key reactions responsible for the initiation, amplification, and feedback inhibition of the coagulation cascade (16) as well as platelet aggregation (7). Indeed, several naturally occurring mutations of the prothrombin gene, like prothrombin Frankfurt (17), Salakta (18), Greenville (19), Scranton (20), Copenhagen (21), and Saint Denis (22), affect residues responsible for Na^+ binding (9) and are often associated with bleeding. Furthermore, thrombin can be engineered for optimal anticoagulant activity *in vitro* and *in vivo* by mutating residues linked to Na^+ binding (15, 23–26).

Thrombin and a few other M^+-activated enzymes like Trp synthase (27, 28), pyruvate kinase (29, 30), Hsc70 (31), β-galactosidase (32, 33), and inosine monophosphate dehydrogenase (34) have been the subject of detailed treatments of the kinetics of M^+ activation. At steady state, Na^+ promotes diffusion into the active site and acylation of substrate by thrombin (35–37). The binding affinity is relatively weak, with a K_d in the millimolar range (35) as found for many other M^+-activated enzymes (1–4), and changes significantly with temperature (38–40). However, the kinetics of M^+ binding to M^+-activated enzymes in general remain for the most part unexplored due to the difficulty of resolving rate constants for reactions that likely occur on a very fast time scale (4). In the case of thrombin, earlier studies have suggested that Na^+ binds in a two-step mechanism with a fast phase occurring within the dead time of the spectrometer (2 ms), followed by a slow phase in the 30-ms time scale at 5 °C (41). In the present study, we revisit these earlier observations and address the kinetic mechanism of Na^+ binding to thrombin in more detail. We identify the Trp residues responsible for the spectral changes and the precise mechanism that gives rise to the two-step components of Na^+ binding.

MATERIALS AND METHODS

Site-directed mutagenesis of human thrombin was carried out in a HPC4-modified pNUT expression vector (15, 42), using the QuikChange site-directed mutagenesis kit from Stratagene

* This work was supported in part by National Institutes of Health Grants HL49413, HL58141, and HL73813. The costs of publication of this article were defrayed in part by the payment of page charges. This article must therefore be hereby marked "*advertisement*" in accordance with 18 U.S.C. Section 1734 solely to indicate this fact.

[S] The on-line version of this article (available at http://www.jbc.org) contains supplemental Figs. S1 and S2.

[1] To whom correspondence should be addressed. Tel.: 314-362-4185; Fax: 314-747-5354; E-mail: enrico@wustl.edu.

(La Jolla, CA) as described (9, 39). Expression of thrombin mutants was carried out in baby hamster kidney cells. Mutants were activated with the prothrombinase complex between 40 and 60 min at 37 °C. Enzymes used in the activation were from Enzyme Research (South Bend, IN). Mutants were purified to homogeneity by fast protein liquid chromatography using Resource Q and S columns with a linear gradient from 0.05 to 0.5 M choline chloride (ChCl), 5 mM MES, pH 6, at room temperature. Active site concentrations were determined by titration with hirudin (43). All nine Trp residues of thrombin were mutated to Phe by single-site substitutions. The conservative replacement did not change the kinetic properties of the constructs, which retained activity toward substrates and Na^+ activation comparable with wild-type (data not shown). Murine thrombin was prepared as reported elsewhere (44).

Stopped-flow fluorescence measurements of Na^+ binding to thrombin were carried out with an Applied Photophysics SX20 spectrometer, using an excitation of 280 nm and a cutoff filter at 305 nm. Samples of thrombin at a final concentration of 50 nM were mixed 1:1 with 60-μl solutions of the same buffer (5 mM Tris, 0.1% polyethylene glycol (PEG),[2] pH 8.0, at 15 °C) containing variable amounts of NaCl (up to 400 mM) kept at constant ionic strength of 400 mM with ChCl. The baseline was measured with 400 mM ChCl in the mixing syringe. Each trace was determined in quadruplicate. Na^+ binding studies were carried out for wild-type thrombin in the temperature range 5–35 °C. The pH was precisely adjusted at room temperature to obtain the value of 8.0 at the desired temperature. Tris buffer has a pK_a of 8.06 at 25 °C and a temperature coefficient of $\Delta pK_a/\Delta T$ of −0.027 (45). These properties ensured buffering over the entire temperature range examined.

The fluorescence increase observed upon Na^+ binding has an initial rapid phase that cannot be resolved within the dead time (<0.5 ms) of the spectrometer, followed by a single exponential slow phase with a k_{obs} that decreases as $[Na^+]$ increases (see "Results"). The total change in fluorescence calculated from the sum of the amplitudes of the fast and slow phases coincides with the value of F determined by equilibrium measurements of intrinsic fluorescence. The value of F as a function of $[Na^+]$ was fit according to Equation 1 (39)

$$F = \frac{F_0 + F_1 K_{app}[Na^+]}{1 + K_{app}[Na^+]} \quad \text{(Eq. 1)}$$

where F_0 and F_1 are the values of F in the absence and under saturating $[Na^+]$ and K_{app} is the apparent equilibrium association constant for Na^+ binding (see below). The value of F_0 corresponds to the base-line reading.

The simplest kinetic scheme accounting for the two-step mechanism of Na^+ binding detected by stopped-flow measurements is given by Scheme 1.

$$E^* \underset{k_1}{\overset{k_{-1}}{\rightleftharpoons}} E \overset{K_A}{\Leftrightarrow} E{:}Na^+$$

SCHEME 1

The free enzyme exists in equilibrium between two forms, E^* and E, that interconvert with kinetic rate constants k_1 and k_{-1}. Of these forms, only E can interact with Na^+ with an equilibrium association constant K_A to generate the E:Na^+ form. The fast phase detected by rapid kinetics is due to the binding of Na^+ to E to generate E:Na^+. Analysis of the fast phase was carried out according to Equation 2, which is analogous to Equation 1,

$$F = \frac{F_0 + F_i K_A[Na^+]}{1 + K_A[Na^+]} \quad \text{(Eq. 2)}$$

where F_i is the value of F under saturating $[Na^+]$ ($F_i < F_1$) and K_A is the intrinsic equilibrium association constant for Na^+ binding. The slow phase is due to the interconversion between E^* and E with an observed rate constant as shown in Equation 3.

$$k_{obs} = k_1 + k_{-1}\frac{1}{1 + K_A[Na^+]} \quad \text{(Eq. 3)}$$

The value of k_{obs} is expected to decrease with increasing $[Na^+]$ from $k_1 + k_{-1}$ ($[Na^+] = 0$) to k_1 ($[Na^+] = \infty$). Analysis of k_{obs} yields k_1, k_{-1}, and a value of K_A that is independent from that derived from analysis of the amplitude of the fast phase according to Equation 2. In the event of a mutation that abrogates the fast phase, the effect of Na^+ binding can still be detected from measurements of k_{obs} (see "Results"). The alternative two-step mechanism as shown in Scheme 2

$$E \overset{K_A}{\Leftrightarrow} E{:}Na^+ \underset{k_1}{\overset{k_{-1}}{\rightleftharpoons}} E^*{:}Na^+$$

SCHEME 2

where a slow isomerization follows the rapid binding of Na^+ leads to an observed rate constant as shown in Equation 4.

$$k_{obs} = k_{-1} + k_1\frac{K_A[Na^+]}{1 + K_A[Na^+]} \quad \text{(Eq. 4)}$$

In this case, the value of k_{obs} is expected to increase with increasing $[Na^+]$ from k_{-1} ($[Na^+] = 0$) to $k_1 + k_{-1}$ ($[Na^+] = \infty$). Hence, the dependence of k_{obs} on $[Na^+]$ is of diagnostic value and rules out Scheme 2 in favor of Scheme 1 (see "Results").

There is a relationship between the *apparent* equilibrium association constant K_{app} derived from Equation 1 and the *intrinsic* equilibrium association constant K_A derived from Equation 2 or 3. The value of K_{app} can also be derived from equilibrium titrations of intrinsic fluorescence (35, 39–41, 46, 47) or linkage studies (38, 46, 48). The value of K_A, on the other hand, can only be derived from rapid kinetic studies. Because of the presence of E, E^*, and E:Na^+ in Scheme 1, at equilibrium one has (49) Equation 5.

$$K_{app} = \frac{K_A}{1 + \frac{k_{-1}}{k_1}} = \frac{K_A}{1 + r} \quad \text{(Eq. 5)}$$

The parameter $r = [E^*]/[E]$ measures the population of E^* relative to E. Under conditions where $r \ll 1$ and the free form is

[2] The abbreviations used are: PEG, polyethylene glycol; MES, 4-morpholineethanesulfonic acid.

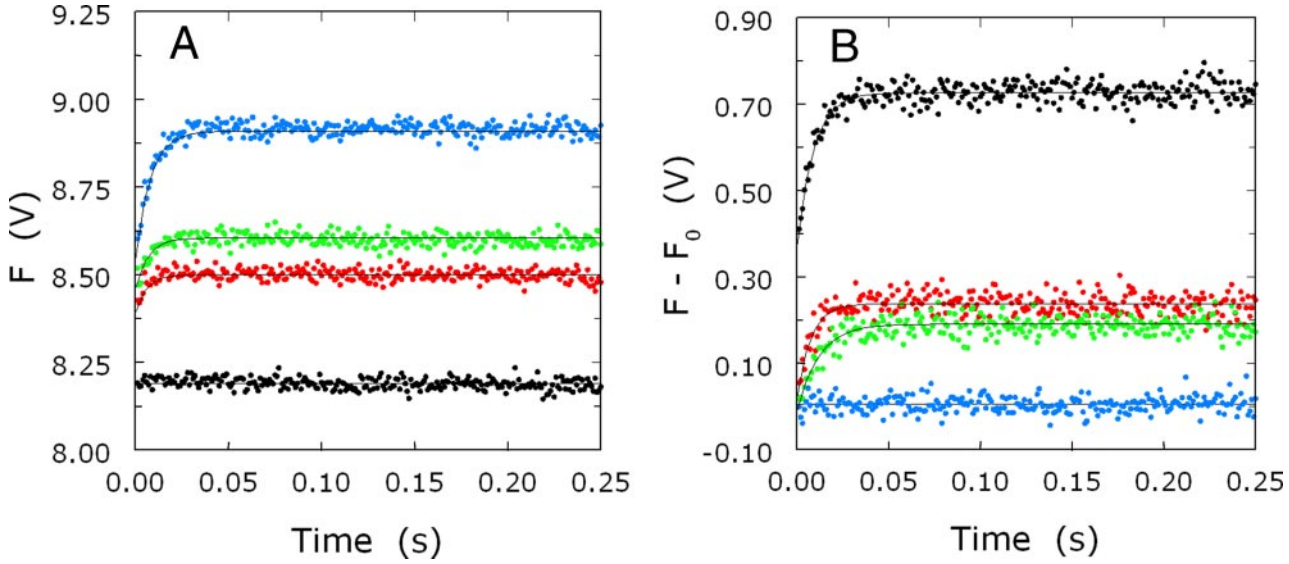

FIGURE 1. *A*, kinetic traces of Na^+ binding to human thrombin in the 0–250-ms time scale. Shown are the traces obtained at 0 (*black circles*), 5 (*red circles*), 10 (*green circles*), and 50 (*blue circles*) mM Na^+. Notice how the binding of Na^+ obeys a two-step mechanism, with a fast phase completed within the dead time (<0.5 ms) of the spectrometer, followed by a single-exponential slow phase. The k_{obs} for the slow phase decreases with increasing [Na^+] (see also Fig. 2), as is evident from the plot. Experimental conditions were 50 nM thrombin, 5 mM Tris, 0.1% PEG, pH 8.0, at 15 °C. The [Na^+] was changed by keeping the ionic strength constant at 400 mM with ChCl. Continuous lines were drawn using the expression $a\{1 - \exp(-k_{obs}t)\} + b$ with best-fit parameter values: *black circles*, $a = 0 \pm 0$ V, $k_{obs} = 0 \pm 0\ s^{-1}$, $b = 8.19 \pm 0.01$ V; *red circles*, $a = 0.11 \pm 0.02$ V, $k_{obs} = 170 \pm 10\ s^{-1}$, $b = 8.39 \pm 0.02$ V; *green circles*, $a = 0.15 \pm 0.02$ V, $k_{obs} = 150 \pm 10\ s^{-1}$, $b = 8.46 \pm 0.02$ V; *blue circles*, $a = 0.37 \pm 0.01$ V, $k_{obs} = 130 \pm 10\ s^{-1}$, $b = 8.54 \pm 0.01$ V. *B*, kinetic traces of Na^+ binding to thrombin wild type and mutants in the 0–250-ms time scale expressed relative to the base-line value F_0 to enable comparison. Shown are the traces obtained at 200 mM Na^+ for human thrombin (*black circles*), mutants W141F (*red circles*), and W215F (*green circles*). Also shown, as a control, is the trace obtained at 200 mM Na^+ for murine thrombin (*blue circles*), which is devoid of Na^+ activation. Notice how mutation of Trp-141 and Trp-215 essentially abolishes the fast phase seen in the wild type (see *panel A*) and reduces significantly the total fluorescence change associated with Na^+ binding (see also Fig. 3 and Table 2). Experimental conditions were 50 nM thrombin, 5 mM Tris, 0.1% PEG, pH 8.0, at 15 °C. Continuous lines were drawn using the expression $a\{1 - \exp(-k_{obs}t)\}$ with best-fit parameter values: *black circles*, $a = 0.36 \pm 0.02$ V, $k_{obs} = 111 \pm 7\ s^{-1}$, $b = 0.37 \pm 0.02$ V; *red circles*, $a = 0.21 \pm 0.02$ V, $k_{obs} = 84 \pm 8\ s^{-1}$, $b = 0.02 \pm 0.02$ V; *green circles*, $a = 0.20 \pm 0.01$ V, $k_{obs} = 130 \pm 10\ s^{-1}$, $b = -0.01 \pm 0.01$ V; *blue circles*, $a = 0 \pm 0$ V, $k_{obs} = 0 \pm 0\ s^{-1}$, $b = 0.00 \pm 0.01$ V.

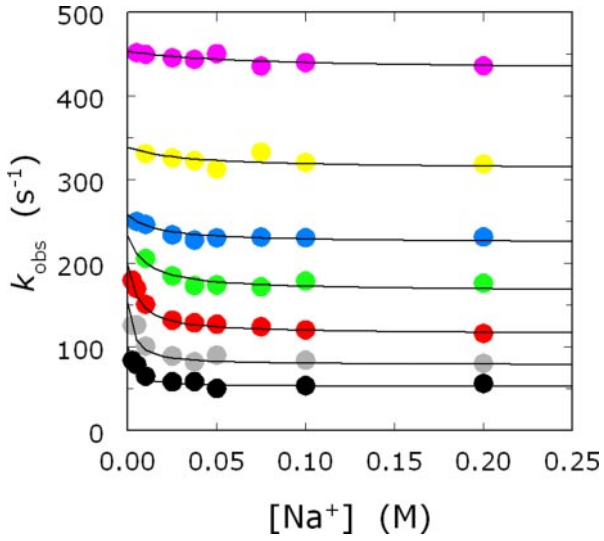

FIGURE 2. **Values of k_{obs} for the slow phase of fluorescence increase due to Na^+ binding to thrombin (see Fig. 1) as a function of [Na^+] in the temperature range 5–35 °C.** Shown are the results pertaining to 5 (*black circles*), 10 (*gray circles*), 15 (*red circles*), 20 (*green circles*), 25 (*blue circles*), 30 (*yellow circles*), and 35 (*magenta circles*) °C. Experimental conditions were 50 nM thrombin, 5 mM Tris, 0.1% PEG, pH 8.0. The [Na^+] was changed by keeping the ionic strength constant at 400 mM with ChCl. Continuous lines were drawn according to Equation 3 under "Materials and Methods" with best-fit parameter values listed in Table 1.

essentially all *E*, the value of K_{app} coincides with K_A. However, under conditions where *r* is significant, a sizable fraction of free thrombin exists in the *E** form and the value of K_{app} underestimates the true Na^+ binding affinity K_A. Hence, it is very important to know how *r* changes under conditions of interest to correctly interpret Na^+ binding in terms of the process that converts *E* to *E*:Na^+.

The temperature dependence of K_{app}, K_A, and *r* yields the thermodynamic parameters associated with the underlying processes according to Equation 6 (39)

$$-\ln K = \frac{\Delta H_0}{R}\frac{1}{T} - \frac{\Delta S_0}{R} + \frac{\Delta C_P}{R}\left(1 - \frac{T_0}{T} - \ln\frac{T}{T_0}\right) \qquad \text{(Eq. 6)}$$

where *K* is K_{app}, K_A, or *r*, ΔH_0 and ΔS_0 are the enthalpy and entropy changes at the reference temperature $T_0 = 298.15$ K, ΔC_P is the heat capacity change, *R* the gas constant, *T* the absolute temperature. The van't Hoff plot of $-\ln K$ *versus* $1/T$ is linear when $\Delta C_P = 0$ and curves upward when $\Delta C_P < 0$.

RESULTS

Na^+ binding to human thrombin gives rise to a significant increase in intrinsic fluorescence (35, 39–41, 46, 47). The change occurs in two steps, clearly revealed by stopped-flow measurements (Fig. 1*A*). A fast phase, whose amplitude increases with [Na^+], occurs within the dead time of the spectrometer (<0.5 ms) and is followed by a single-exponential slow phase whose k_{obs} decreases with increasing [Na^+]. Control experiments run with murine thrombin, an enzyme devoid of Na^+ activation (44), show no change in fluorescence even at 200 mM Na^+ (Fig. 1*B*). The dependence of k_{obs} on [Na^+] is hyperbolic (Fig. 2) and is consistent with the mechanism

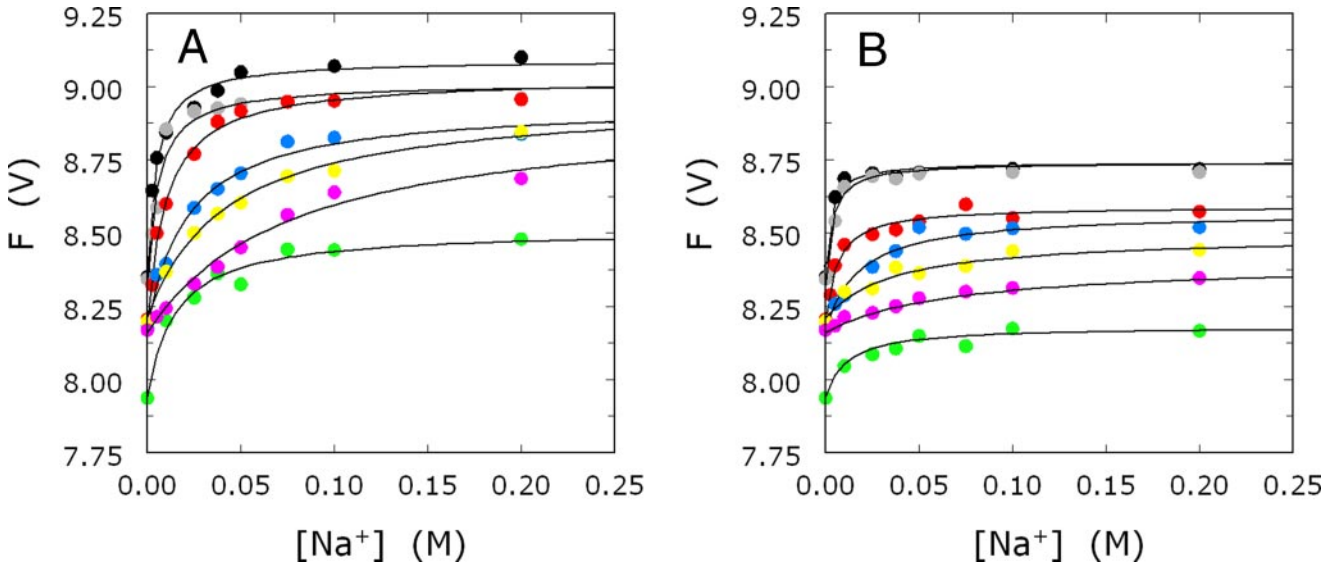

FIGURE 3. *A*, Na^+ binding curves of thrombin obtained from the total change in intrinsic fluorescence measured as the sum of the amplitudes of the fast and slow phases determined by stopped-flow kinetics (see Fig. 1). Shown are the results pertaining to 5 (*black circles*), 10 (*gray circles*), 15 (*red circles*), 20 (*green circles*), 25 (*blue circles*), 30 (*yellow circles*), and 35 (*magenta circles*) °C. Experimental conditions were 50 nM thrombin, 5 mM Tris, 0.1% PEG, pH 8.0. The [Na^+] was changed by keeping the ionic strength constant at 400 mM with ChCl. Continuous lines were drawn according to Equation 1 under "Materials and Methods", with best-fit parameter values listed in Table 1. *B*, Na^+ binding curves of thrombin obtained from the amplitude of the fast phase of fluorescence increase determined by stopped-flow kinetics (see Fig. 1). Shown are the results pertaining to 5 (*black circles*), 10 (*gray circles*), 15 (*red circles*), 20 (*green circles*), 25 (*blue circles*), 30 (*yellow circles*), and 35 (*magenta circles*) °C. Experimental conditions were 50 nM thrombin, 5 mM Tris, 0.1% PEG, pH 8.0. The [Na^+] was changed by keeping the ionic strength constant at 400 mM with ChCl. Continuous lines were drawn according to Equation 2 under "Materials and Methods" with best-fit parameter values listed in Table 1.

TABLE 1

Fluorescence and Na^+ binding parameters for wild-type thrombin as a function of temperature

The parameters F_0, F_i, and F_1 defining $\Delta F_i = F_i - F_0$ and $\Delta F_t = F_1 - F_0$ were derived from analysis of the data in Fig. 3, *A* and *B*, using Equations 1 and 2 under "Materials and Methods." The values of K_{app} were derived from analysis of the data in Fig. 3*A* according to Equation 1. The values of K_A were derived from analysis of the data in Fig. 3*B* according to Equation 2, and Fig. 2 according to Equation 3, together with the values of k_1 and k_{-1}. *r* is the ratio k_{-1}/k_1. Note how the values of K_{app} and K_A obtained independently obey Equation 5 under "Materials and Methods."

T	F_0	F_i	F_1	$\Delta F_i/F_0$	$\Delta F_t/F_0$	K_{app}	K_A	k_1	k_{-1}	*r*
°C	*V*	*V*	*V*	%	%	M^{-1}	M^{-1}	s^{-1}	s^{-1}	
5	8.36 ± 0.02	8.74 ± 0.02	9.09 ± 0.02	4.5	8.7	220 ± 20	370 ± 40	52 ± 2	48 ± 2	0.92
10	8.32 ± 0.03	8.74 ± 0.03	9.01 ± 0.03	5.0	8.3	180 ± 20	300 ± 40	78 ± 4	75 ± 4	0.96
15	8.19 ± 0.01	8.59 ± 0.02	9.03 ± 0.01	4.9	10.3	100 ± 10	160 ± 20	115 ± 3	83 ± 6	0.72
20	7.94 ± 0.03	8.18 ± 0.03	8.51 ± 0.03	3.0	7.1	68 ± 7	90 ± 9	166 ± 4	65 ± 8	0.39
25	8.18 ± 0.03	8.57 ± 0.03	8.94 ± 0.03	4.8	9.3	46 ± 5	57 ± 4	224 ± 4	34 ± 4	0.15
30	8.21 ± 0.02	8.49 ± 0.02	8.96 ± 0.02	3.4	9.1	24 ± 2	28 ± 2	312 ± 4	27 ± 8	0.086
35	8.16 ± 0.02	8.40 ± 0.02	8.93 ± 0.02	2.9	9.4	13 ± 1	15 ± 1	431 ± 10	23 ± 4	0.053

depicted in Scheme 1 and Equation 3. That supports the conclusion that, in the absence of Na^+, thrombin exists in equilibrium between two conformations, *E** and *E*, and that only *E* can be converted to the *E*:Na^+ form. The binding of Na^+ to *E* gives rise to the fast phase. The slow phase detected by stopped-flow measurements is the result of the interconversion between *E** and *E* that takes place on a time scale of milliseconds.

The sum of the amplitudes of the slow and fast phases changes hyperbolically with [Na^+] (Fig. 3*A*) and recapitulates the behavior observed by intrinsic fluorescence measurements at equilibrium (35, 39–41, 46, 47). Analysis of such curves in the temperature range 5–35 °C enables determination of K_{app} from Equation 1 (Table 1). A van't Hoff plot of the K_{app} values is shown in Fig. 4 and reveals a curvature conducive to the presence of a heat capacity change of −500 cal/mol/K, consistent with previous results (38–40). Analysis of the amplitude of the fast phase as a function of [Na^+] (Fig. 3*B*) according to Equation 2 enables the determination of K_A (Table 1). These values of K_A are practically identical to those derived independently from analysis of k_{obs} as a function of [Na^+] according to Equation 3 (Fig. 2), which also enables resolution of k_1 and k_{-1} (Table 1). The van't Hoff plot of the K_A values is curved, as for K_{app}, due to a heat capacity change of −500 cal/mol/K (Fig. 4). This proves that the heat capacity change reported previously for the values of K_{app} (38–40) reflects an intrinsic property of Na^+ binding to thrombin and is not the result of the pre-existing equilibrium between *E* and *E**. In fact, from the definition of K_{app} in Equation 5, it can be seen that the *E*-*E** equilibrium gives rise to an apparent heat capacity change when the value of *r* changes with temperature, even if no heat capacity change is associated with K_A and/or *r*. The direct determination of K_A from rapid kinetic data resolves the transition from *E* to *E*:Na^+ in Scheme 1 and decouples this process from the linked equilibrium between *E* and *E**. The temperature dependence of K_A then offers direct validation of the heat capacity change associated with Na^+ binding as a basic thermodynamic property of thrombin (38–40).

Binding of Na^+ is characterized by a large enthalpy change of

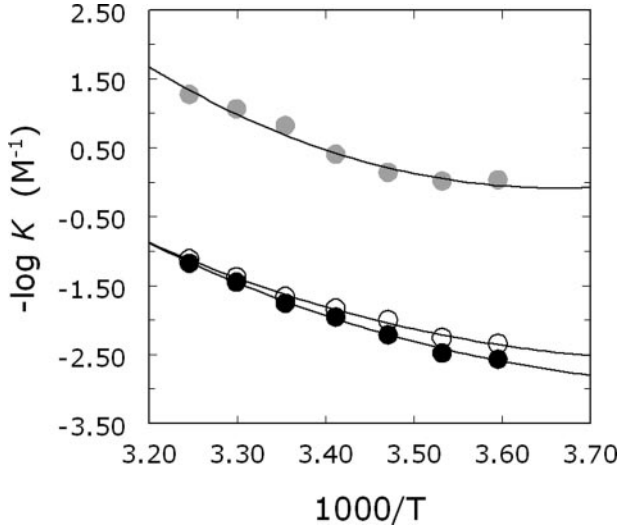

FIGURE 4. **van't Hoff plots of Na^+ binding to thrombin.** Shown are the values of K_{app} (*open circles*) and K_A (*black circles*) obtained from stopped-flow kinetics in the temperature range 5–35 °C (see Table 1). The plot is curved in both cases, signaling the presence of a heat capacity change. Also shown is the temperature dependence of −log *r* (*gray circles*, dimensionless units), measuring the equilibrium between *E* and *E** in Scheme 1 (see Table 1). This parameter too is associated with significant curvature in the plot, signaling a large heat capacity change. Experimental conditions were 5 mM Tris, 0.1% PEG, pH 8.0. Continuous lines were drawn according to Equation 6 under "Materials and Methods" with best-fit parameter values: *open circles*, $\Delta H_0 = -18.9 \pm 0.9$ kcal/mol, $\Delta S_0 = -56 \pm 3$ cal/mol/K, $\Delta C_P = -500 \pm 100$ cal/mol/K; *black circles*, $\Delta H_0 = -21.5 \pm 0.9$ kcal/mol, $\Delta S_0 = -64 \pm 3$ cal/mol/K, $\Delta C_P = -500 \pm 100$ cal/mol/K; *gray circles*, $\Delta H_0 = -23 \pm 2$ kcal/mol, $\Delta S_0 = -81 \pm 8$ cal/mol/K, $\Delta C_P = -900 \pm 300$ cal/mol/K.

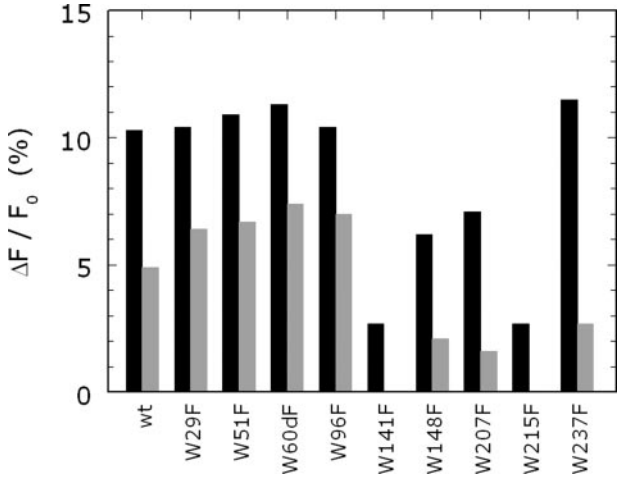

FIGURE 5. **Fluorescence change induced by Na^+ binding to wild type and the Phe mutants of all nine Trp residues of human thrombin.** Shown are the values listed in Table 2 for the total change in intrinsic fluorescence measured as $F_1 - F_0$ (*black bars*) or the amplitude of the fast phase measured as $F_i - F_0$ (*gray bars*). All values are expressed as % change relative to F_0. Experimental conditions were 50 nM thrombin, 5 mM Tris, 0.1% PEG, pH 8.0, at 15 °C. The [Na^+] was changed by keeping the ionic strength constant at 400 mM with ChCl.

−22 kcal/mol that is compensated by a large entropy loss of −64 cal/mol/K (Fig. 4). The enthalpy change is due to formation of the six ligating interactions in the coordination shell that also involve four buried water molecules (3, 4, 9). The entropy change reflects the uptake and ordering of water molecules within the channel embedding the primary specificity pocket and the active site linked to the occupancy of the Na^+ site (9). As a result of the enthalpy-entropy energetic compensation, the binding affinity of Na^+ is relatively weak (K_d in the mM range), as seen for many other M^+-activated enzymes (3, 4). An important consequence of the large enthalpy change is that the value of K_A becomes only about 10 M^{-1} at 37 °C, which implies that under physiologic conditions of temperature and [NaCl] = 140 mM thrombin is only 60% bound to Na^+, as first documented in 1992 (35). This makes thrombin optimally poised for allosteric regulation *in vivo*, where the Na^+-bound and Na^+-free forms are targeted toward procoagulant and anticoagulant roles, respectively (7, 10).

It is of particular importance to structurally assign the spectral changes linked to Na^+ binding to thrombin. Trp-215 in the aryl binding site has been identified as a major fluorophore responsible for the spectral change (48), but a rigorous test of the contribution of all nine Trp residues of thrombin has not been carried out. Previous studies investigated the role of Trp-60d, Trp-96, Trp-148, Trp-207, and Trp-215 with Phe substitutions, but the analysis involved the activity toward thrombin substrates and not Na^+ binding (50). Fig. 5 shows the fluorescence enhancement due to Na^+ binding for the Phe mutants of all nine Trp residues of thrombin. The Phe mutations of the nine Trp residues of thrombin cause few, if any, changes in the kinetic and equilibrium properties of the enzyme toward Na^+ (Table 2). The Trp → Phe substitution therefore provides an optimal adiabatic perturbation of the indole moiety and probes selectively the changes monitored by fluorescence spectroscopy. The data in Fig. 5 refer to the total fluorescence change, $F_1 - F_0$ in Equation 1 (*black bars*) or the amplitude of the fast phase, $F_i - F_0$ in Equation 2 (*gray bars*), both relative to the base-line value F_0. The 10% total increase in fluorescence observed for wild type is retained by five Trp mutants, namely, W29F, W51F, W60dF, W96F, and W237F. Two mutants, W148F and W207F, experience >30% loss in total fluorescence change. On the other hand, W141F and W215F lose >70% of the total fluorescence change. Inspection of the fast component of the fluorescence change is even more informative. This phase monitors directly Na^+ binding to *E* to generate the *E*:Na^+ form. In the wild type, the amplitude of the fast phase, $F_i - F_0$ (see Table 1 and Figs. 1*B* and 3*B*), is about half the amplitude of the total fluorescence change, $F_1 - F_0$ (see Table 1 and Figs. 1*A* and 3*A*). The amplitude of the fast phase is perturbed in all Trp mutants, even when the total fluorescence change is the same as for wild type (Figs. 1 and 5). Because Trp residues are distributed over the entire structure of thrombin, and their distance from the bound Na^+ ranges from 13 (Trp-215) to 35 (Trp-51) Å, binding of Na^+ to *E* likely elicits effects well beyond the immediate environment of the Na^+ site and perturbs the structure of thrombin as a whole. This is in agreement with recent functional mapping of the Na^+-induced allosteric transition of thrombin (51). The amplitude of the fast phase increases significantly relative to wild type for the W29F, W51F, W60dF, and W96F mutants. On the other hand, the amplitude decreases significantly for W148F, W207F, and W237F and completely disappears for W141F and W215F. Hence, Trp-215 but also Trp-141 are major reporters of the process of Na^+ binding to thrombin. Trp-148, Trp-207, and Trp-237 also contribute to

TABLE 2
Fluorescence and Na^+ binding parameters for wild-type thrombin and mutants

	F_o	F_i	F_1	$\Delta F_i/F_o$	$\Delta F_1/F_o$	K_{app}	K_A	k_1	k_{-1}	r	D^a
	V	*V*	*V*	%	%	M^{-1}	M^{-1}	s^{-1}	s^{-1}		Å
wt	8.19 ± 0.01	8.59 ± 0.02	9.03 ± 0.01	4.9	10.3	100 ± 10	160 ± 20	115 ± 3	83 ± 6	0.72	
W29F	8.17 ± 0.02	8.69 ± 0.02	9.02 ± 0.02	6.4	10.4	58 ± 6	85 ± 7	126 ± 4	74 ± 4	0.59	24
W51F	8.15 ± 0.01	8.70 ± 0.02	9.04 ± 0.01	6.7	10.9	100 ± 10	170 ± 30	114 ± 3	87 ± 6	0.76	35
W60dF	8.13 ± 0.01	8.73 ± 0.03	9.05 ± 0.01	7.4	11.3	89 ± 6	140 ± 10	132 ± 2	77 ± 9	0.58	21
W96F	8.13 ± 0.03	8.70 ± 0.03	8.98 ± 0.03	7.0	10.4	70 ± 10	110 ± 10	133 ± 2	69 ± 2	0.52	27
W141F	8.02 ± 0.01	8.02 ± 0.01	8.24 ± 0.01	0.0	2.7	110 ± 10	170 ± 10	79 ± 1	40 ± 9	0.51	23
W148F	8.18 ± 0.02	8.35 ± 0.02	8.69 ± 0.02	2.1	6.2	81 ± 8	130 ± 10	95 ± 2	72 ± 4	0.76	21
W207F	8.15 ± 0.01	8.28 ± 0.02	8.73 ± 0.01	1.6	7.1	120 ± 10	190 ± 10	89 ± 2	78 ± 2	0.88	23
W215F	8.12 ± 0.01	8.12 ± 0.01	8.34 ± 0.01	0.0	2.7	59 ± 8	110 ± 10	118 ± 3	81 ± 7	0.69	13
W237F	8.14 ± 0.02	8.36 ± 0.01	9.08 ± 0.01	2.7	11.5	110 ± 10	170 ± 10	101 ± 2	68 ± 3	0.67	30

[a] Distance from the Cε2 atom of the Trp residue to the bound Na^+ in the crystal structure of the Na^+-bound form 1SG8 (9). All parameters were derived as shown in Table I. Note how the values of K_{app} and K_A obtained independently obey Equation 5 under "Materials and Methods."

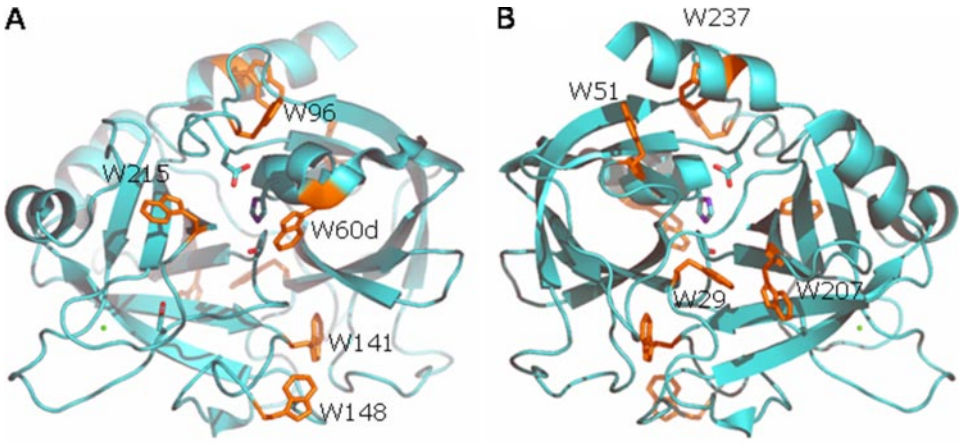

FIGURE 6. ***Ribbon plot* of thrombin in the Na^+-bound form, portraying the structure 1SG8 (9) with the active site in the front (*A*) or rotated 180° along the *y*-axis (*B*).** Shown are the side chains of the catalytic residues His-57, Asp-102, and Ser-195 and the side chain of Asp-189. Na^+ is rendered as a *green ball*. The nine Trp residues of the enzyme are shown with their side chains in *orange*. The contribution of these residues to the fluorescence change induced by Na^+ binding is shown in Fig. 5 and Table 2. The A chain was removed for clarity.

the spectral change, whereas Trp-29, Trp-51, Trp60d, and Trp-96 produce changes that oppose those of the other fluorophores because their replacement to Phe actually enhances the fluorescence change due to Na^+ binding.

DISCUSSION

The results presented here expand and clarify the scenario offered by the only previous investigation of Na^+ binding to thrombin using rapid kinetics (41). The earlier study was carried out at 5 °C and ionic strength values of 0.3 and 2.0 M, using 500 nM thrombin. Two phases were identified, as shown in Fig. 1*A*, but no dependence of k_{obs} on [Na^+] could be detected below 500 mM [Na^+]. This made interpretation of the results particularly cumbersome and did not support the use of simple mechanisms like Scheme 1 or Scheme 2. The study, however, uncovered the pre-existing equilibrium between *E* and *E** as depicted in Scheme 1. There are several reasons why our results, and especially the dependence of k_{obs} on [Na^+], differ in part from those reported previously. The SX20 spectrometer is a much improved version of the SX17 model used previously (41) and features a shorter dead time and higher signal resolution and stability. The thrombin concentration used in our measurements (50 nM) did not result in any photobleaching, thereby eliminating the need to correct for the effect when fitting experimental data. When using 500 nM thrombin, as in the previous study (41), we did observe significant photobleaching that affected base-line stability, reproducibility, and extent of fluorescence change (see supplemental data). When we further reduced the thrombin concentration down to 5 nM, the results lacked the optimal reproducibility observed at 50 nM. Significant photobleaching was acknowledged in the previous study (41), but not resolved. The previous study was carried out at 5 °C, where condensation in the cell is very significant and must be eliminated with constant N_2 flushing. We found that the temperature range of 15–25 °C is optimal to resolve the range of k_{obs} linked to Na^+ binding. Last, but not least, the pK_a of Tris buffer at 5 °C is 8.60 (45), which makes it problematic to buffer a solution at pH 7.4 as used in the previous study (41).

Our results add mechanistic significance to previous studies of Na^+ binding because of the use of Phe mutations of all nine Trp residues of thrombin. The fast phase of fluorescence increase directly linked to the transition from *E* to *E*:Na^+ in Scheme 1 is affected in all Phe mutants, vouching for a global effect of Na^+ binding on thrombin structure. The contributions of single Trp residues are not additive, lending support to the hypothesis that some of the environments in which they reside may be coupled allosterically. The coupling may ensure propagation of long-range effects originating at the Na^+ site via a limited number of structural conduits. Trp-141 and Trp-215 make a large contribution to the fluorescence change induced by Na^+ binding, and their mutation to Phe abrogates the fast phase completely. This implies that the environments of Trp-141 and Trp-215 change in the *E** to *E* conversion, and more drastically in the conversion of *E* to *E*:Na^+. The important role of Trp-215 has been reported before (48). This is the closest Trp residue to the bound Na^+ (13 Å) and defines most of the aryl binding site involved in substrate recognition (5, 9, 52). The importance of Trp-141 is unanticipated. However, recent structures of thrombin document a flip in the indole ring of Trp-141 in the absence of Na^+ similar to that observed for

Trp-215 (49). Trp-141 is buried in a strategic location between the autolysis loop and exosite I, and its linkage with the bound Na^+, situated 23 Å away, vouches for a pivotal role in communicating changes from the Na^+ site to exosite I (Fig. 6). Among the other residues that contribute to the fluorescence change and the fast phase, Trp-148 is located in the middle of the highly flexible autolysis loop, 21 Å away from the bound Na^+, and is 62% exposed to solvent (52), whereas Trp-207 is completely buried in the back of the catalytic chain, 23 Å away from the bound Na^+, and in hydrophobic contact with Trp-29 and residues of the A chain (Fig. 6). Because of their proximity, Trp-207 and Trp-29 may function as a single fluorophore and/or quench each other. It is interesting that the Phe mutation of Trp-29 enhances the amplitude of the fast phase, as though changes affecting Trp-207 are better reported in the absence of Trp-29. A similar scenario can be envisioned for Trp-51 and Trp-237 (Fig. 6), whose hydrophobic coupling may result in overlapping spectral effects with Trp-51 actually hindering the full response of Trp-237 to Na^+ binding. Finally, the effects seen with the highly solvent-exposed Trp-60d and Trp-96 (Fig. 6) suggest that these residues may be quite flexible and capable of probing different environments that reduce the fluorescence response to Na^+ binding.

It is of interest to correlate the new information arising from stopped-flow measurements of the mechanism of Na^+ binding to thrombin with existing structural data. The three species in Scheme 1 portray thrombin in the Na^+-free (*E* and *E**) and Na^+-bound (*E*:Na^+) forms, and the data presented here demonstrate that Na^+ binds to thrombin in a two-step mechanism consistent with Scheme 1. The activation effect of Na^+ on thrombin has very clear kinetic signatures and specifically involves an increase in k_{cat} and a decrease in K_m (35–37, 49, 53, 54). Such a "modifier" effect on k_{cat} has long been known to be of diagnostic value (55) and unequivocally proves the existence of two active forms in equilibrium, one Na^+ free with low k_{cat} and one Na^+ bound with high k_{cat} (4, 49). *E* and *E*:Na^+ in Scheme 1 are the two active forms of thrombin that account for the dependence of k_{cat} on [Na^+] and correspond to the slow (*E*) and fast (*E*:Na^+) forms originally defined by Wells and Di Cera (35). The structures of these two forms have been solved recently (9). Basic differences between them involve the orientation of Asp-189 in the primary specificity pocket, Ser-195 in the active site, and the reorganization of a water network that connects the Na^+ site to the active site Ser-195 located 16 Å away. The orientation of Asp-189 in the fast form optimizes docking of the guanidinium group of Arg at the P1 position of substrate. The Oγ atom of Ser-195 in the fast form is within H-bonding distance of the catalytic His-57. The H-bond is required for efficient catalysis (56) and is broken in the slow form. The network of water molecules ensures the long-range communication between the bound Na^+ and the active site that is at the basis of thrombin allostery. The increase in the number and ordering of water molecules linked to Na^+ binding also explains the large entropy loss and negative heat capacity change associated with this process. Unfortunately, the differences between the slow and fast forms reported recently (9) do not involve Trp residues that contribute to the spectral changes linked to Na^+ binding. Either such changes are too subtle to be unraveled under the constrained environment of a crystal lattice or available structures of the slow and/or fast forms are not representative of the full landscape of conformational transitions induced by Na^+ binding. Indeed, functional mapping of the slow → fast transition suggests a more global involvement of thrombin residues (51).

Structural assignments for the *E** form are equally problematic. In a previous study on the kinetics of Na^+ binding to thrombin, *E** was interpreted as an "inactive" slow form unable to bind Na^+ and substrate or inhibitors at the active site (41). The conclusion was drawn from data showing that the binding of inhibitors to thrombin was also linked to increases in intrinsic fluorescence and obeyed a mechanism similar to that of Na^+ binding (41). The hypothesis of *E** being an inactive conformation of the slow form, as originally suggested by Lai *et al.* (41), has gained prominence recently in the context of several structures of inactive forms of thrombin in the Na^+-free form that have appeared in the literature. These structures differ drastically from the active slow form *E* (9, 57) and share disorder or collapse of the Na^+ site and steric blockage of the active site (49, 58–61). We have recently shown (62) that these inactive structures are likely the result of mutations introduced in the enzyme (58, 59) and/or artifacts of crystal packing (49, 60, 61). A recent structure of thrombin obtained in the absence of inhibitors and salts appears to be a genuine inactive slow form, devoid of artifactual effects due to mutations in the Na^+ site or crystal packing (62). The structure has the Na^+ site obliterated by the side chain of Arg-187 and the active site occluded by the repositioning of the side chains of Trp-215 and Arg-221a. The drastic movement of Trp-215 would do justice to the dominant role played by this residue in the fluorescence changes reported in our study. However, even this structure lacks significant changes around all other Trp residues. Hence, evidence that thrombin can assume an inactive slow form under crystallographic conditions is strong (62), but the connection with the functional properties of the enzyme in solution remains weak. The kinetic signatures of Na^+ activation do not require inactive conformations of thrombin and indeed refute (4, 49) simplistic "alternative" models based on the equilibrium of active and inactive forms (61).

The data presented in this study vouch for *E** being a form of thrombin unable to bind Na^+ and not necessarily inactive toward substrates or inhibitors. In fact, a conformation of thrombin with the pore of entry to the Na^+ binding site (4, 39) occluded would fit the description of *E** and would still retain activity toward substrates and inhibitors. Whether inactive conformations of thrombin in the slow form exist in solution remains to be demonstrated by future studies of rapid kinetics involving the library of Trp mutants presented here in order to structurally assign the observed spectral changes and confirm that they have the same origin as those linked to Na^+ binding. However, even if future studies in solution prove that *E** is indeed an inactive slow form, then its possible physiologic role should be clarified. Based on the data in Fig. 5, *E** represents <1% of the population of thrombin molecules at 37 °C, which raises questions about its possible functional role *in vivo*. This conundrum does not apply to the active slow form, which contributes 40% of the thrombin molecules *in vivo* and whose anti-

coagulant role is well established (7, 10, 15). Nonetheless, *E** carries considerable mechanistic significance for Na^+ binding to thrombin and may become populated under the effect of mutations or conditions that involve allosteric effectors to be identified. In addition, *E** is an intriguing new variable to be taken into consideration when studying Na^+ binding to other clotting factors and M^+-activated enzymes.

REFERENCES

1. Suelter, C. H. (1970) *Science* **168,** 789–795
2. Evans, H. J., and Sorger, G. J. (1966) *Annu. Rev. Plant. Physiol.* **17,** 47–76
3. Di Cera, E. (2006) *J. Biol. Chem.* **281,** 1305–1308
4. Page, M. J., and Di Cera, E. (2006) *Physiol. Rev.* **86,** 1049–1092
5. Bode, W. (2006) *Blood Cells Mol. Dis.* **36,** 122–130
6. Davie, E. W., and Kulman, J. D. (2006) *Semin. Thromb. Hemostasis* **32,** Suppl. 1, 3–15
7. Di Cera, E. (2003) *Chest* **124,** 11S–17S
8. Di Cera, E., Guinto, E. R., Vindigni, A., Dang, Q. D., Ayala, Y. M., Wuyi, M., and Tulinsky, A. (1995) *J. Biol. Chem.* **270,** 22089–22092
9. Pineda, A. O., Carrell, C. J., Bush, L. A., Prasad, S., Caccia, S., Chen, Z. W., Mathews, F. S., and Di Cera, E. (2004) *J. Biol. Chem.* **279,** 31842–31853
10. Dang, O. D., Vindigni, A., and Di Cera, E. (1995) *Proc. Natl. Acad. Sci. U. S. A.* **92,** 5977–5981
11. Myles, T., Yun, T. H., Hall, S. W., and Leung, L. L. (2001) *J. Biol. Chem.* **276,** 25143–25149
12. Nogami, K., Zhou, Q., Myles, T., Leung, L. L., Wakabayashi, H., and Fay, P. J. (2005) *J. Biol. Chem.* **280,** 18476–18487
13. Yun, T. H., Baglia, F. A., Myles, T., Navaneetham, D., Lopez, J. A., Walsh, P. N., and Leung, L. L. (2003) *J. Biol. Chem.* **278,** 48112–48119
14. Ayala, Y. M., Cantwell, A. M., Rose, T., Bush, L. A., Arosio, D., and Di Cera, E. (2001) *Proteins* **45,** 107–116
15. Dang, Q. D., Guinto, E. R., and Di Cera, E. (1997) *Nat. Biotechnol.* **15,** 146–149
16. Page, M. J., and Di Cera, E. (2006) *Thromb. Haemostasis* **95,** 920–921
17. Degen, S. J., McDowell, S. A., Sparks, L. M., and Scharrer, I. (1995) *Thromb. Haemostasis* **73,** 203–209
18. Miyata, T., Aruga, R., Umeyama, H., Bezeaud, A., Guillin, M. C., and Iwanaga, S. (1992) *Biochemistry* **31,** 7457–7462
19. Henriksen, R. A., Dunham, C. K., Miller, L. D., Casey, J. T., Menke, J. B., Knupp, C. L., and Usala, S. J. (1998) *Blood* **91,** 2026–2031
20. Sun, W. Y., Smirnow, D., Jenkins, M. L., and Degen, S. J. (2001) *Thromb. Haemostasis* **85,** 651–654
21. Stanchev, h., Philips, M., Villoutreix, B. O., Aksglaede, L., Lethagen, S., and Thorsen, S. (2006) *Thromb. Haemostasis* **95,** 195–198
22. Rouy, S., Vidaud, D., Alessandri, J. L., Dautzenberg, M. D., Venisse, L., Guillin, M. C., and Bezeaud, A. (2006) *Br. J. Haematol.* **132,** 770–773
23. Gibbs, C. S., Coutre, S. E., Tsiang, M., Li, W. X., Jain, A. K., Dunn, K. E., Law, V. S., Mao, C. T., Matsumura, S. Y., Mejza, S. J., Paborsky, L. R., and Leung, L. L. K. (1995) *Nature* **378,** 413–416
24. Cantwell, A. M., and Di Cera, E. (2000) *J. Biol. Chem.* **275,** 39827–39830
25. Tsiang, M., Paborsky, L. R., Li, W. X., Jain, A. K., Mao, C. T., Dunn, K. E., Lee, D. W., Matsumura, S. Y., Matteucci, M. D., Coutre, S. E., Leung, L. L., and Gibbs, C. S. (1996) *Biochemistry* **35,** 16449–16457
26. Gruber, A., Cantwell, A. M., Di Cera, E., and Hanson, S. R. (2002) *J. Biol. Chem.* **277,** 27581–27584
27. Woehl, E., and Dunn, M. F. (1999) *Biochemistry* **38,** 7118–7130
28. Woehl, E., and Dunn, M. F. (1999) *Biochemistry* **38,** 7131–7141
29. Mesecar, A. D., and Nowak, T. (1997) *Biochemistry* **36,** 6803–6813
30. Mesecar, A. D., and Nowak, T. (1997) *Biochemistry* **36,** 6792–6802
31. O'Brien, M. C., and McKay, D. B. (1995) *J. Biol. Chem.* **270,** 2247–2250
32. Xu, J., McRae, M. A., Harron, S., Rob, B., and Huber, R. E. (2004) *Biochem. Cell Biol.* **82,** 275–284
33. Neville, M. C., and Ling, G. N. (1967) *Arch. Biochem. Biophys.* **118,** 596–610
34. Digits, J. A., and Hedstrom, L. (1999) *Biochemistry* **38,** 2295–2306
35. Wells, C. M., and Di Cera, E. (1992) *Biochemistry* **31,** 11721–11730
36. Ayala, Y. M., and Di Cera, E. (2000) *Protein Sci.* **9,** 1589–1593
37. Krem, M. M., Prasad, S., and Di Cera, E. (2002) *J. Biol. Chem.* **277,** 40260–40264
38. Guinto, E. R., and Di Cera, E. (1996) *Biochemistry* **35,** 8800–8804
39. Prasad, S., Wright, K. J., Roy, D. B., Bush, L. A., Cantwell, A. M., and Di Cera, E. (2003) *Proc. Natl. Acad. Sci. U. S. A.* **100,** 13785–13790
40. Griffon, N., and Di Stasio, E. (2001) *Biophys. Chem.* **90,** 89–96
41. Lai, M. T., Di Cera, E., and Shafer, J. A. (1997) *J. Biol. Chem.* **272,** 30275–30282
42. Guinto, E. R., Vindigni, A., Ayala, Y. M., Dang, Q. D., and Di Cera, E. (1995) *Proc. Natl. Acad. Sci. U. S. A.* **92,** 11185–11189
43. Dang, Q. D., and Di Cera, E. (1994) *J. Protein Chem.* **13,** 367–373
44. Bush, L. A., Nelson, R. W., and Di Cera, E. (2006) *J. Biol. Chem.* **281,** 7183–7188
45. Stoll, V. S., and Blanchard, J. S. (1990) *Methods Enzymol.* **182,** 24–38
46. Ayala, Y., and Di Cera, E. (1994) *J. Mol. Biol.* **235,** 733–746
47. De Filippis, V., De Dea, E., Lucatello, F., and Frasson, R. (2005) *Biochem. J.* **390,** 485–492
48. Arosio, D., Ayala, Y. M., and Di Cera, E. (2000) *Biochemistry* **39,** 8095–8101
49. Carrell, C. J., Bush, L. A., Mathews, F. S., and Di Cera, E. (2006) *Biophys. Chem.* **121,** 177–184
50. Bell, R., Stevens, W. K., Jia, Z., Samis, J., Cote, H. C. F., MacGillivray, R. T. A., and Nesheim, M. E. (2000) *J. Biol. Chem.* **275,** 29513–29520
51. Mengwasser, K. E., Bush, L. A., Shih, P., Cantwell, A. M., and Di Cera, E. (2005) *J. Biol. Chem.* **280,** 23997–27003
52. Bode, W., Turk, D., and Karshikov, A. (1992) *Protein Sci.* **1,** 426–471
53. Vindigni, A., and Di Cera, E. (1996) *Biochemistry* **35,** 4417–4426
54. Orthner, C. L., and Kosow, D. P. (1980) *Arch. Biochem. Biophys.* **202,** 63–75
55. Botts, J., and Morales, M. (1953) *Trans Faraday Soc.* **49,** 696–707
56. Fuhrmann, C. N., Daugherty, M. D., and Agard, D. A. (2006) *J. Am. Chem. Soc.* **128,** 9086–9102
57. Pineda, A. O., Savvides, S. N., Waksman, G., and Di Cera, E. (2002) *J. Biol. Chem.* **277,** 40177–40180
58. Carter, W. J., Myles, T., Gibbs, C. S., Leung, L. L., and Huntington, J. A. (2004) *J. Biol. Chem.* **279,** 26387–26394
59. Pineda, A. O., Chen, Z. W., Caccia, S., Cantwell, A. M., Savvides, S. N., Waksman, G., Mathews, F. S., and Di Cera, E. (2004) *J. Biol. Chem.* **279,** 39824–39828
60. Papaconstantinou, M. E., Carrell, C. J., Pineda, A. O., Bobofchak, K. M., Mathews, F. S., Flordellis, C. S., Maragoudakis, M. E., Tsopanoglou, N. E., and Di Cera, E. (2005) *J. Biol. Chem.* **280,** 29393–29396
61. Johnson, D. J., Adams, T. E., Li, W., and Huntington, J. A. (2005) *Biochem. J.* **392,** 21–28
62. Pineda, A. O., Chen, Z. W., Bah, A., Garvey, L. C., Mathews, F. S., and Di Cera, E. (2006) *J. Biol. Chem.* **281,** 32922–32928